Identification of a key molecular regulator of liver metastasis in human pancreatic carcinoma using a novel quantitative model of metastasis in NOD/SCID/γ_c^{null} (NOG) mice

HIROSHI SUEMIZU[1*], MAKOTO MONNAI[1,2*], YASUYUKI OHNISHI[1], MAMORU ITO[1], NORIKAZU TAMAOKI[1] and MASATO NAKAMURA[1,3,4]

[1]Biomedical Research Department, Central Institute for Experimental Animals, 1430 Nogawa, Miyamae, Kawasaki, Kanagawa 216-0001; [2]Chugai Research Institute for Medical Science, Inc., 200 Kajiwara, Kamakura, Kanagawa 247-8530; [3]Department of Pathology, Tokai University School of Medicine, Bohseidai, Isehara, Kanagawa 259-1193; [4]Department of Pathology, Tokai University School of Medicine, Hachioji Hospital, 1838 Ishikawa, Hachioji, Tokyo 192-0032, Japan

Received December 27, 2006; Accepted February 14, 2007

Abstract. We developed a reliable new model system for assaying liver metastasis using NOD/SCID/γ_c^{null} (NOG) mice. Seven human pancreatic cancer cell lines were examined for their ability to form diverse metastatic foci in the livers of NOD/SCID and NOG mice. Capan-2 and PL45 showed no metastasis when seeded at up to 10^5 cells in both strains, and no BxPC-3 metastasis was observed in NOD/SCID mice. The NOD/SCID mouse model detected liver metastasis only in the AsPC-1 cell line when inoculated with $>10^3$ cells. In contrast, when inoculated with only 10^2 MIA PaCa-2, AsPC-1 and PANC-1 cells, liver metastasis was evident in 71.4% (5/7), 57.1% (4/7) and 37.5% (3/8) of the NOG mice, respectively. Capan-1 and BxPC-3 cells metastasized when seeded at 10^3 cells in 50% (5/10) and in 12.5% (1/8) of the mice, respectively. Using the NOG mouse model system, we established a highly metastatic cell line, liver metastasized-BxPC-3 (LM-BxPC-3), from liver metastatic foci formed by the relatively poorly metastatic parental BxPC-3 cell line. The gene expression profiles of parental and LM-BxPC-3 cells were compared, and we identified forty-five genes that were either upregulated or downregulated >4-fold in the LM-BxPC-3 cell line. We validated 9 candidate protein-coding sequences, and examined the correlation between their expression pattern and the *in vivo* liver metastatic potential of all 7 pancreatic cancer cell lines. Only S100A4 expression correlated with the ability to form liver metastases, as evaluated in our quantitative model of metastasis in NOG mice. These results suggested that S100A4 is a key regulator of liver metastasis in pancreatic cancer, and demonstrated the feasibility of using the quantitative metastasis model to search for and develop new anti-cancer therapies and novel drugs against this and other key molecules.

Correspondence to: Dr Hiroshi Suemizu, Central Institute for Experimental Animals, 1430 Nogawa, Miyamae, Kawasaki, Kanagawa 216-0001, Japan
E-mail: suemizu@ciea.or.jp

*Contributed equally

Key words: NOD/SCID/γ_c^{null} mice, NOG mice, liver metastasis, human pancreatic cancer

Introduction

Pancreatic cancer is one of the most aggressive human cancers. The inability to detect early-stage carcinoma, and the lack of effective systemic therapies for treating the disease are significant factors in the rapid death and low survival rate of patients with pancreatic cancer. Even after extensive curative pancreatectomy, patients have a poor prognosis due to the high rate of liver metastasis in pancreatic cancer. Metastasis is a complex cascade of events that involves interactions between cancer cells and multiple host factors (1). Information on the pathobiology of metastatic pancreatic cancer, and elucidation of the underlying molecular mechanisms are urgently needed in order to develop novel and effective therapeutic approaches to treatment. New strategies for treating metastatic pancreatic cancer will also require the development of appropriate animal models for studying their effectiveness. Attempts to demonstrate the liver metastatic potential of human cancers have been carried out using intrasplenic injections of cancer cells into immunocompromised mice, such as athymic nude mice or severe combined immunodeficient (SCID) mice (2-4). However, metastatic rates in these systems were usually low, despite the fact that a large number of cells were injected ($>1x10^6$ cells).

Recently, we developed NOD/SCID/γ_c^{null} (NOG) mice by backcrossing IL-2 receptor γ-chain deficient (γ_c^{null}) mice (5)

to NOD/Shi-SCID mice (6). NOG mice have no lymphocytes (neither T nor B) or natural killer (NK) cells, and have impaired dendritic cell function. The severe immunodeficiency in these mice allowed for high engraftment efficiency of human hematopoietic stem cells, leading to full lineage differentiation in NOG mice (7). Moreover, when compared with NOD/Shi-SCID mice, NOG mice were a superior xenotransplantation system for the engraftment of human cancer cells (8). In a stable and reproducible animal model of metastasis, differences in liver metastatic potential *in vivo* can be reliably assessed. Metastatic potential is due, in part, to differential gene expression. In this context, analysis of gene expression of pancreatic cancer cells with different metastatic potential, in terms of incidence and grade, is extremely relevant to our understanding of the mechanism of pancreatic cancer metastasis.

In this study, intrasplenic injections of NOG mice were used to select a metastatic cell subpopulation derived from the human pancreatic cancer cell line, BxPC-3, allowing us to derive a highly metastatic variant cell line, LM-BxPC-3. We explored genes whose expression was associated with *in vivo* metastatic potential by analyzing the expression profiles of ~47,000 genes in parental BxPC-3 and LM-BxPC-3 cells using a high-density oligonucleotide array. From this analysis, nine candidate genes that had altered expression profiles in LM-BxPC-3 cells were selected. Subsequent to expression analysis of these nine genes in 6 other human pancreatic cancer cell lines, we identified a gene, S100A4, whose expression level correlated closely with the development of liver metastatic behavior.

Materials and methods

Cells. AsPC-1, BxPC-3, Capan-1, Capan-2, MIA PaCa-2, PANC-1, and PL45 were obtained from the American Type Culture Collection (Manassas, VA). BxPC-3, Capan-2 and PL45 were maintained in RPMI-1640 (Sigma, St. Louis, MO) supplemented with 10% fetal bovine serum (FBS, HyClone, UT, USA). MIA PaCa-2 and PANC-1 were maintained in Dulbecco's modified Eagle's medium (DMEM) with 10% FBS. DMEM containing 20 or 15% FBS was used for AsPC-1 and Capan-1, respectively. Cells were incubated in a humidified (37˚C, 5% CO_2) incubator and passaged on reaching 80% confluence.

In vivo growth and liver metastasis assay. We bred NOD/SCID (NOD/ShiJic-SCID) and NOG (NOD/ShiJic-SCID with γ_c^{null}) mice and used them at the age of 7-9 weeks, in accordance with institutional guidelines. For evaluation of the growth potential of individual cell lines *in vivo*, NOG mice were given a subcutaneous (s.c) injection of 10^4 tumor cells suspended in 0.1 ml of serum-free medium and 0.1 ml of Matrigel (BD Biosciences, Bedford, MA). Apparent tumors were measured weekly. Experimental liver metastases were generated by intrasplenic injection of cancer cells and splenectomy (9). The mice were sacrificed 6-8 weeks later, and liver metastases were enumerated immediately, without fixation. We defined the ratio of tumor to total liver surface area (T/L score) using Image processing and analysis in Java software (ImageJ version 1.33, http://rsb.info.nih.gov/ij/).

Establishment of a highly metastatic pancreatic cell line. NOG mice were given an intrasplenic injection of $1x10^5$ BxPC-3. The mice were euthanized 6 weeks after injection, and the livers were removed and subjected to gross examination. Metastatic foci with diameters >2 mm were collected and cut into 1-mm^3 cubes. Foci were dispersed into single cells in a solution of trypsin-EDTA (IBL Co., Ltd. Takasaki, Japan). Contamination with non-human cells (mouse-derived cells) was checked by PCR using the following primers: forward primer, 5'-TGTAGGTACTAACACTGGCTCGTGTGACA A-3' and reverse primer, 5'-GGTGTTGAAGGTCTCAAAC ATGATCTGTA-3'. This set of primers amplifies not only human ß-actin gene, but also mouse ß-actin gene (247 bp and 273 bp, respectively). Short tandem repeat (STR) analysis was carried out to check for cross contamination of other pancreatic cancer cell lines using the following markers: D5S818, D13S317, D7S820, and D16S539. Primer information is available at the UniSTS database on the NCBI web site (http://www.ncbi.nlm.nih.gov/). The liver metastasized cell line that was isolated in this manner, LM-BxPC-3, was expanded and injected into a new cohort of mice as described above to confirm its metastatic ability.

Oligonucleotide array hybridization; data analysis and validation. Total cellular RNA was obtained from 90% confluent cultures of BxPC-3 and LM-BxPC-3 cells using the RNeasy mini kit (Qiagen K.K. Tokyo, Japan). Gene expression was analyzed using the HG-U133A Plus 2 GeneChip array (Affymetrix Inc., Santa Clara, CA). Signal intensity for each transcript (background subtracted and adjusted for noise) and detection call (present, absent, or marginal) was determined using Microarray Suite software 5.0 (Affymetrix Inc.). Scatter plot and fold-change analyses were performed using the Data mining tool (Affymetrix Inc.). Genes with altered expression were pinpointed with the local-pooled-error test (10) with a false discovery rate p of 0.05, indicating a statistically significant difference (either increased or decreased) in their expression in the LM-BxPC-3 line, compared with the parental BxPC-3 line. To validate GeneChip expression data, reverse transcription-polymerase chain reaction (RT-PCR) was performed using the same RNA samples as in the GeneChip array experiment. We confirmed that nine genes had significantly different expression levels in LM-BxPC-3 cells, compared with parental BxPC-3 cells. RT-PCR using primer sets specific for these nine genes (sequences available upon request) was conducted under the following conditions: 95˚C for 10 sec; 23 to 32 cycles at 95˚C for 5 sec; and 62˚C for 31 sec. For quantitative analysis, an aliquot of cDNA was added to the Master mix of SYBR-Premix Ex Taq™ (Perfect real time, Takara Bio Inc., Shiga, Japan), and quantitative gene expression data was acquired using an ABI PRISM 7700 sequence detection system (Applera Corporation, Applied Biosystems, CA). RT-PCR of GAPDH RNA was used to standardize the results.

Protein expression of selected genes was carried out by immunoblot analysis. Primary antibodies used were rabbit polyclonal anti-S100A4 antibody at a dilution of 1:100 (DakoCytomation, Kyoto, Japan), and goat polyclonal anti-GAPDH antibody at a dilution of 1:300 (Santa Cruz

Biotechnology, Inc. Santa Cruz, CA). Secondary antibodies were horseradish peroxidase-conjugated anti-rabbit Ig 1:500 (Amersham Biosciences, Tokyo, Japan), and anti-goat Ig (Bethyl Inc., Montgomery, TX) at a dilution of 1:500. Immunoblots were developed using the ECL Western blotting detection system (Amersham Biosciences) and Hyperfilm ECL (Amersham Biosciences).

Plasmid constructs, transfection and derivation of stable cell lines. The full-length cDNA encoding S100A4 was cloned into the pCXN2 vector, which possesses a neomycin-selectable marker (11). Transfection of pCXN2-S100A4 was performed by Magnetofection (Oz Biosciences, France) according to the manufacturer's instructions. Two days after transfection, 500 μg/ml of neomycin (Invitrogen Corp., Carlsbad, CA) was added to the cultures and maintained until cell death in the cultures ceased.

Statistical analyses. All statistical analyses were performed using StatView, version 5.0 (SAS Institute, Tokyo, Japan). The significance of variances was analyzed as required by the Kruskal-Wallis test, Tukey-Kramer test and Mann-Whitney U test. A p-value <0.05 was considered to indicate significant differences.

Results

In vivo model of liver metastasis. Seven human pancreatic cancer cell lines were examined for their ability to form diverse metastatic foci in the liver of NOD/SCID and NOG mice. The incidences of liver metastases in NOG mice were far higher than those in NOD/SCID mice (Table I). Capan-2 and PL45 showed no metastasis when seeded up to 10^5 cells in both strains, and no BxPC-3 metastasis was observed in NOD/SCID mice. The NOD/SCID mouse model detected liver metastasis only for the AsPC-1 cell line when inoculated with $>10^3$ cells. In contrast, when inoculated with only 10^2 MIA PaCa-2, AsPC-1 and PANC-1 cells, liver metastasis was evident in 71.4-37.5% of the NOG mice. Representative images of liver metastases are shown in Fig. 1. The incidence of metastasis of Capan-1 or BxPC-3 cells was greatly reduced when fewer numbers of cells were inoculated into the NOG mice. In contrast, apparent metastases were evident in >50% of NOG mice inoculated with $1x10^2$ AsPC-1 or MIA PaCa-2 cells (Table I). Thus, the occurrence of metastatic lesions in the livers of NOG mice was dose dependent, reproducible, and apparent over a wide range of logarithmic values. The metastatic potential of the different cell lines can be ranked as follows: MIA PaCa-2 > AsPC-1 > PANC-1 >

Table I. Liver metastasis after intrasplenic injection of human pancreatic cancer cells.

Cell line	Cell dose (cells/head)	Number of animals with liver metastasis[a] (metastasis/total)		Metastatic score in NOG mice	
		NOD/SCID	NOG	%T/L[b] (mean±SD)	Liver surface area[c] (mm^2, mean±SD)
MIA PaCa-2	$1x10^4$	0/10 (0.0%)	10/10 (100.0%)	60.6±13.9	1056.0±338.0
	$1x10^3$	0/7 (0.0%)	5/6 (83.3%)	ND	ND
	$1x10^2$	0/6 (0/0%)	5/7 (71.4%)	ND	ND
AsPC-1	$1x10^4$	8/9 (88.9%)	9/9 (100.0%)	48.2±12.3	434.4±77.6
	$1x10^3$	2/8 (25.0%)	8/8 (100.0%)	ND	ND
	$1x10^2$	0/6 (0.0%)	4/7 (57.1%)	ND	ND
PANC-1	$1x10^4$	0/10 (0.0%)	8/8 (100.0%)	26.6±11.3	374.0±68.5
	$1x10^3$	0/6 (0.0%)	6/8 (75.0%)	ND	ND
	$1x10^2$	0/7 (0.0%)	3/8 (37.5%)	ND	ND
Capan-1	$1x10^4$	0/10 (0.0%)	9/10 (90.0%)	15.6±5.3	425.6±38.5
	$1x10^3$	0/10 (0.0%)	5/10 (50.0%)	ND	ND
	$1x10^2$	0/8 (0.0%)	0/8 (0.0%)	ND	ND
BxPC-3	$1x10^5$	0/8 (0.0%)	8/8 (100.0%)	ND	ND
	$1x10^4$	0/8 (0.0%)	1/8 (12.5%)	0.0±0.0	409.4±37.3
Capan-2	$1x10^5$	0/8 (0.0%)	0/8 (0.0%)	ND	ND
	$1x10^4$	ND	0/10 (0.0%)	0.0±0.0	426.7±39.1
PL45	$1x10^5$	0/8 (0.0%)	0/8 (0.0%)	ND	ND
	$1x10^4$	ND	0/10 (0.0%)	0.0±0.0	395.0±36.1

[a]Liver metastasis was evaluated 6 weeks after inoculation of $1x10^3$, 10^4 and 10^5 cancer cells, and 8 weeks after inoculation of 10^2 cancer cells. [b]All liver images showing liver metastases in response to injection of $1x10^4$ cancer cells were used to calculate the percent tumor occupancy in the liver (T/L). [c]The surface area of the liver was calculated using all liver images obtained from mice which were injected with $1x10^4$ cancer cells. ND, not done.

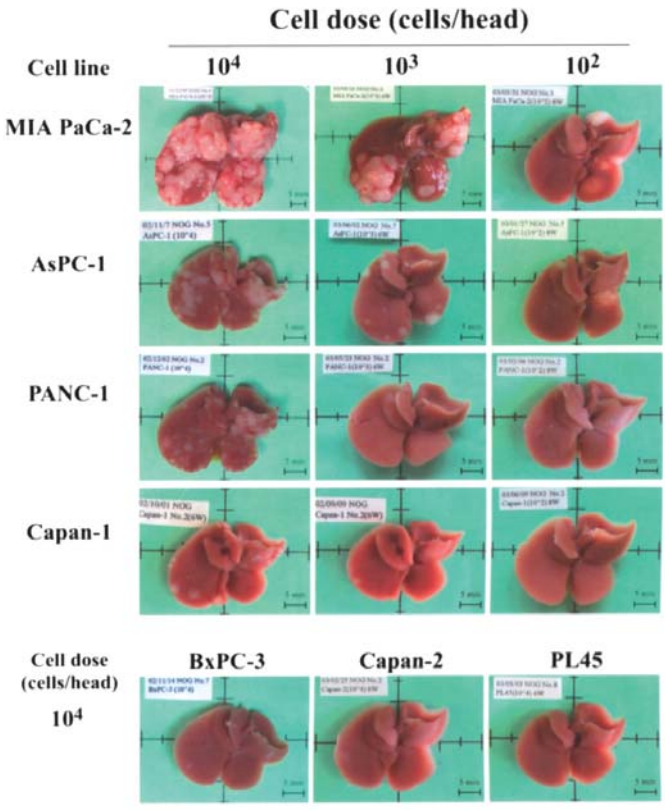

Figure 1. Representative gross findings of liver metastases of human pancreatic cancer cell lines. Seven human pancreatic cancer cell lines: MIA PaCa-2, AsPC-1, PANC-1, Capan-1, BxPC-3, Capan-2 and PL45 were intrasplenically implanted into NOG mice. The mice were sacrificed 6 weeks later, and liver metastases were enumerated immediately, without prior fixation.

Capan-1 > BxPC-3 > Capan-2 and PL45. The liver metastatic potential of 7 individual pancreatic cancer cell lines in NOG mice was quantitated as the T/L score (Table I). The ranking of metastatic potential was quantitatively reproduced using T/L score analysis. Six weeks after $1x10^4$ cells were implanted, the T/L score of each cell line was as follows: MIA PaCa-2, 60.6%; AsPC-1, 48.2%; PANC-1, 26.6%; and Capan-1, 15.6% (Table I). The overall surface area of livers inoculated with pancreatic cancer cells was not significantly different from that of normal (non-inoculated) NOG mouse livers, with the exception of livers inoculated with MIA PaCa-2 cells (data not shown). The surface area of the livers of NOG mice inoculated with $1x10^4$ MIA PaCa-2 cells was double that of the livers inoculated with other cell lines (Table I).

To evaluate *in vivo* growth activities, $1x10^4$ pancreatic cancer cells were injected subcutaneously into NOG mice. The tumor volume for MIA PaCa-2 was the largest among the seven cell lines. In contrast, PL45 cells did not form tumors in NOG mice. The doubling times of tumors derived from AsPC-1, BxPC-3, Capan-1 and Capan-2, were not statistically different (data not shown), and subcutaneous tumorigenicity did not correlate with metastatic potential. These results indicated that the liver metastatic potential of human pancreatic cancer cells in NOG mice is not directly related to tumor growth.

Establishment and characterization of a highly metastatic pancreatic cell line. Parental BxPC-3 cells (Fig. 2b) showed poor metastatic capability in our liver metastasis model using NOG mice, but a few visible tumor foci consistently developed (Fig. 2a and c). We isolated cells from these foci,

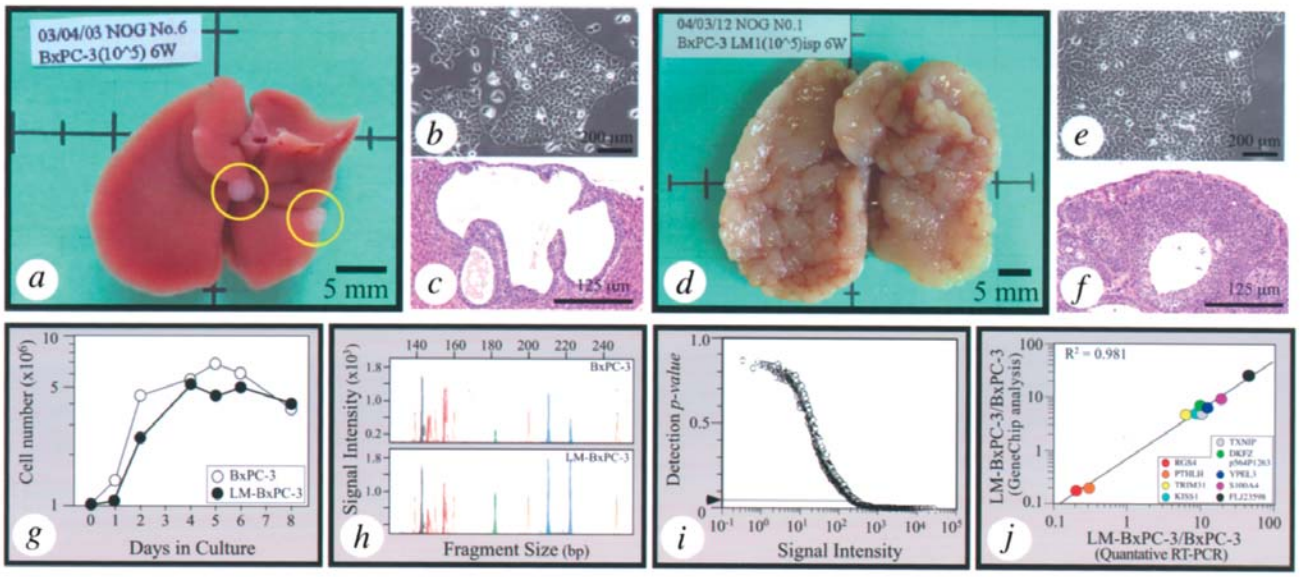

Figure 2. Establishment of a highly metastatic liver cell line. Primary tumors were generated by intrasplenic injection of $1x10^5$ BxPC-3 cells into NOG mice (a-c). Cells from liver metastatic foci (open circles in a) were isolated and designated as LM-BxPC-3. Metastatic ability of the LM-BxPC-3 cell line was evaluated by intrasplenic injection with $1x10^5$ cells (d-f). BxPC-3 and LM-BxPC-3 cells were seeded onto a culture dish after trypsinization, cultured for the indicated number of days and then enumerated after suspension under a microscope (g). STR analysis was carried out to check for cross contamination of other pancreatic cancer cell lines (h). Four microsatellite loci D5S818, D13S317, D7S820, and D16S539 were examined with NED, VIC, 6-FAM and PET fluorescent dye-labeled primers. The relationship between signal intensity and detection p-value was averaged for each of the 100 genes. Arrowhead on the Y-axis indicates a detection p-value of 0.05 (i). The expression levels of nine genes were validated by comparing GeneChip data with the results of quantitative RT-PCR (j).

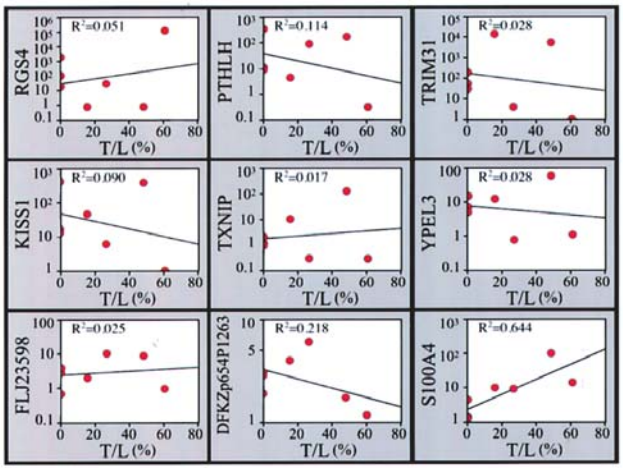

Figure 3. Correlation analysis between gene expression levels and liver metastatic potential. The expression levels of 9 selected genes were analyzed in 7 pancreatic cancer cell lines. The liver metastatic ability is represented as the percentage of tumor occupation in the liver (T/L).

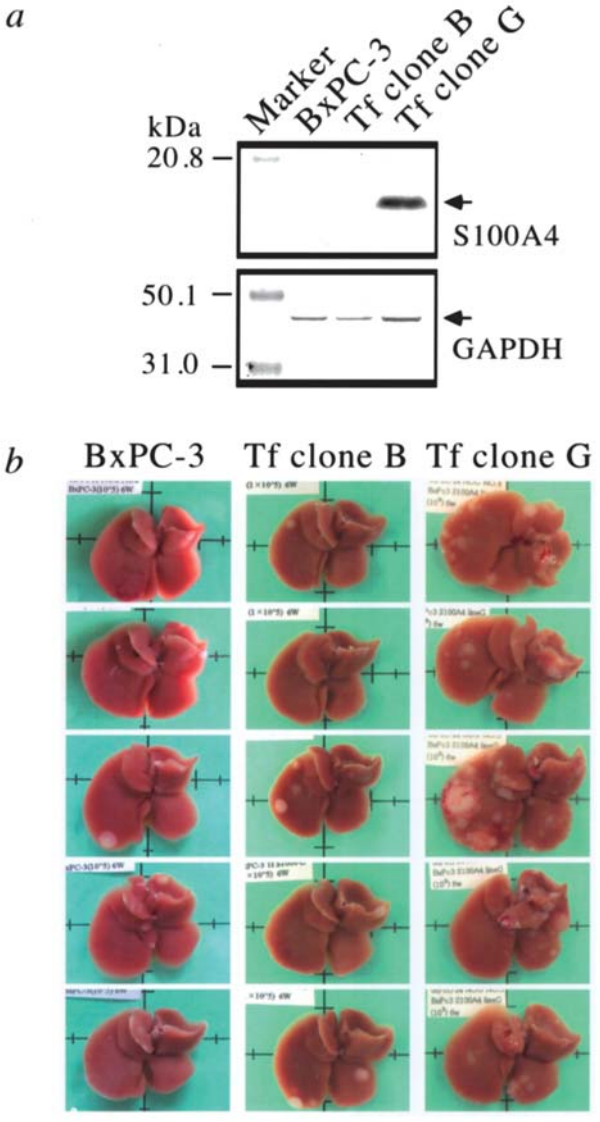

Figure 4. S100A4 enhances liver metastatic potential of human pancreatic cancer cells. Expression levels of S100A4 and GAPDH in BxPC-3 cells, and S100A4-transfectants B and G. Immunoblots were probed with a rabbit polyclonal anti-S100A4 antibody (a, top), and a goat polyclonal anti-GAPDH antibody (a, bottom). Gross analysis of liver metastases in mice injected with BxPC-3 (b, left), S100A4-transfectant clone B (b, center) and clone G (b, right). Cells were intrasplenically implanted, mice were sacrificed 6 weeks later, and liver metastases were enumerated immediately, without prior fixation.

and designated them 'LM (Liver-Metastasized)-BxPC-3' cells (Fig. 2e). After a short period in culture, $1x10^5$ LM-BxPC-3 cells were injected into NOG mice. In contrast to the parental cell line, we observed aggressive metastasis at 6 weeks when LM-BxPC-3 cells were injected into NOG mice (Fig. 2d and f). When we compared the growth characteristics of parental BxPC-3 and LM-BxPC-3 cells, we observed no major difference in *in vitro* growth activity (Fig. 2g). To eliminate the possibility of cross contamination with other pancreatic cancer cell lines, we carried out STR analysis of 4 microsatellite loci. Both cell lines had the same genetic profile at all microsatellite markers examined (D5S818, 143/143 bp; 13S317, 182/182 bp; D7S820, 210/222 bp; D16S539, 146/156 bp; Fig. 2h). No other pancreatic cancer cell lines had this type of genetic profile (data not shown).

Gene expression profiling of the metastatic phenotype and validation of the data. We performed oligonucleotide microarray analysis (Affymetrix, Human Genome U133 Plus 2.0 array) to identify genes that were differentially expressed in BxPC-3 cells and their derivative LM-BxPC-3 cells. Genes were sorted by increasing signal intensity, and then the average signal intensity and detection p-value were averaged for each of the 100 genes in the list. The average detection p-value was low for well-expressed genes, but increased for genes with signal intensities <200 (Fig. 2i). Although signal intensities of <200 were variable, they were still useful for comparing highly metastatic LM-BxPC-3 cells with the control parental BxPC-3 cell line. Thus, to avoid overestimating fold changes, and to increase reliability, we set a lower limit of detection at 200 (detection p-value=0.05) and replaced all values of <200 with 200. Among >47,000 total feature sets present on the chip, when parental cells were compared with LM-BxPC-3 cells, statistically significant differences in gene expression (4-fold or greater) were observed with 54 probe sets. The 54 probe sets corresponded to 45 gene sets because the GeneChip we used in this study included multiple probe sets that recognized different regions of the same transcript. All of the genes that had significantly different (>4-fold) expression levels, ranked in order of fold-difference, are listed in Table II. Nine genes had decreased expression levels, whereas 36 genes had increased expression levels in LM-BxPC-3 cells, compared with the parental cell line. To validate the GeneChip data, RT-PCR was performed on two underexpressed genes (RGS4 and PTHLH), and seven overexpressed genes (TRIM31, KISS1, TXNIP, S100A4, YPEL3, FLJ23598 and DFKZp56P1263) in the LM-BxPC-3 line. Real-time RT-PCR was carried out to quantitate the expression of each of these genes. The expression dynamics based on quantitative RT-PCR were in agreement with the GeneChip data (Fig. 2j).

The S100A4 gene is associated with pancreatic cancer liver metastasis. To determine whether the genes identified by

expression profiling of BxPC-3 and LM-BxPC-3 cells were associated with liver metastasis in other pancreatic cancer cell lines, we examined gene expression using quantitative RT-PCR, and liver metastatic potential with the T/L score of each of the other six pancreatic cancer cell lines. For eight of the nine genes, there was no correlation between gene expression and liver metastasis (Fig. 3). However, expression of S100A4 strongly correlated with liver metastasis (R^2=0.644) (Fig. 3). The level of S100A4 protein was analyzed by immunoblot (data not shown), using NIH ImageJ to evaluate signal intensity and GAPDH protein levels as the standard. There was a strong correlation between S100A4 protein level and liver metastasis, as defined by the T/L score, in all seven pancreatic cancer cell lines (R^2=0.739, data not shown).

Effect of S100A4 overexpression on liver metastasis. The S100A4 gene was identified because its expression level correlated closely with liver metastasis. We were interested in the effect of S100A4 overexpression on liver metastatic potential of pancreatic cancer cells. The full-length human S100A4 cDNA was cloned into pCXN2 and transfected into BxPC-3 parental cells. Two neomycin-resistant cell lines were selected, Tf clones G and B, in which S100A4 expression was dramatically increased, or was the same as that in non-transfected parental cells, respectively (Fig. 4a). Both cell lines were implanted intrasplenically into NOG mice to evaluate their *in vivo* liver metastatic potential. Metastatic potential was evaluated by the incidence of liver metastasis and the T/L score (Table III). When NOG mice were inoculated with $1x10^5$ cells and sacrificed 6 weeks later, the incidence of liver metastasis in the mice that received either S100A4-transfectants or non-transfectants (BxPC-3 cells) was 100%. However, the features of liver metastases seemed to be quite different depending on S100A4 expression levels. Typical images are shown in Fig. 4b. The T/L score of each cell line was calculated, and the correlation between S100A4 expression and liver metastatic potential was evaluated. Tf clone G which expressed high levels of S100A4 protein had a significantly higher T/L score compared with the Tf clone B, which was neomycin resistant but had extremely low levels of S100A4 protein and non-transfected parental BxPC-3 cells. Liver metastatic lesions formed reproducibly and semiquantitatively in a dose-dependent manner. On inoculation with $1x10^4$ cells, liver metastasis was evident in only 12.5% of NOG mice that received non-transfected parental BxPC-3 cells, and was never observed in mice that received Tf clone B cells. In contrast, inoculation of $1x10^4$ Tf clone G cells resulted in apparent metastasis in >50% of NOG mice.

Discussion

Several studies using microarrays and serial analysis of gene expression (SAGE) to characterize the molecular biology of pancreatic tumors and pancreatic cancer cell lines have been reported (12-14). While these cell lines from different tumor types may share some features at the molecular level, it is believed that the function of the genes showing similar expression profiles among different cancer cell lines is to promote pancreatic tumorigenesis. We are particularly interested in liver metastasis of pancreatic tumors. In this study, we first examined the *in vivo* biological behavior of seven human pancreatic cancer cell lines. Reproducible *in vivo* evaluation of liver metastatic potential was possible using completely immunocompromised NOG mice developed in our laboratory. The liver metastatic incidence and grade of each of the pancreatic cancer cell lines were quantitatively evaluated, and were dose dependent over a wide range of inoculation doses. To date, ours is the only *in vivo* model for liver metastasis that can evaluate metastatic potential with an inoculation dose of 10^2 cells. Using this system, we succeeded in deriving a highly metastatic cell line from a poorly metastatic parental line in a single *in vivo* passage in the mouse liver. Differentially expressed genes in these two cell lines were identified by global gene expression analysis with Affymetrix oligonucleotide microarrays. To validate whether the differentially expressed genes were involved in liver metastasis of other pancreatic cancer cell lines, we analyzed the correlation between gene expression and *in vivo* liver metastatic ability in 6 pancreatic cancer cell lines. A candidate liver metastasis-related gene, S100A4, was exogenously expressed in a poorly metastatic cell line, and the effect on *in vivo* liver metastasis was evaluated in the NOG mice. These experiments indicated that S100A4, which is a member of the S100 family of calcium-binding proteins, is a strong candidate for genes involved in liver metastasis *in vivo*.

Several models of liver metastasis using intrasplenic injection of cancer cells have been established and characterized using athymic nude mice (15-17). Hematogenous metastasis occurs as a consequence of a well-characterized set of sequential events. These types of metastasis models mimic only those events that occur after entrance of cells into the blood vessels. In most of these model systems, more than one million cancer cells are intrasplenically inoculated into mice to generate liver metastases (3,17-19). It is unlikely, however, that such a large number of cancer cells would enter the liver at one time via the portal vein, and form metastatic foci in patients with pancreatic cancer.

In this study, we demonstrated a high rate of liver metastasis in NOG mice inoculated with small numbers of cancer cells (as low as one hundred cells), and a higher level of liver metastasis in the NOG mouse model than that in NOD/SCID mice. This liver metastasis model using NOG mice is reliable and quantitative, and more closely mimics the *in vivo* conditions in patients with pancreatic cancer. It will also be a valuable tool for exploring new metastasis-related genes using genome-wide gene expression profiles of different cancer cell lines. Several cell lines with a high metastatic potential were established by serial intrasplenic transplantation of cancer cells in order to explore putative genes associated with pancreatic cancer-liver metastasis in patients (17,18). In athymic nude mice, poorly metastatic cells required several passages before they acquired the ability to metastasize. When a poorly metastatic bladder cancer cell line, T24T, was serially passaged through nude mice, the cellular characteristics progressively changed, resulting in an increased pulmonary metastatic load and decreased period of time for metastases to develop (16). In most experiments involving serial passaging, not only metastatic ability, but also cellular characteristics such as

Table II. Differences in gene expression between the human pancreatic cancer cell line BxPC-3 and the highly metastatic derivative LM-BxPC-3.

Probe set ID[a]	Gene[b]	Fold difference[c]	Chromosome[d]
Highly expressed in BxPC-3 parental cells			
204338_s_at	**Regulator of G-protein signalling 4 (RGS4)**	7.5	1q23.3
204337_at	**Regulator of G-protein signalling 4 (RGS4)**	5.7	1q23.3
204339_s_at	**Regulator of G-protein signalling 4 (RGS4)**	4.9	1q23.3
211756_at	**Parathyroid hormone-like hormone (PTHLH)**	4.9	12p12.1-p11.2
1556773_at	**Parathyroid hormone-like hormone (PTHLH)**	4.9	12p12.1-p11.2
206300_s_at	**Parathyroid hormone-like hormone (PTHLH)**	4.9	12p12.1-p11.2
206343_s_at	Neuregulin 1 (NRG1)	4.9	8p21-p12
207526_s_at	Interleukin 1 receptor-like 1 (IL1RL1)	4.6	2q12
231771_at	Gap junction protein, ß 6 (GJB6)	4.3	13q12
211423_s_at	Sterol-C5-desaturase (ERG3 Δ-5-desaturase homolog, fungal)-like (SC5DL)	4.3	11q23.3
212977_at	Chemokine orphan receptor 1	4.0	2q37.3
223779_at	Hypothetical protein MGC10981	4.0	4p16.1
Highly expressed in LM-BxPC-3 cells			
202376_at	Serine (or cysteine) proteinase inhibitor, clade A, member 3 (SERPINA3)	36.8	14q32.1
220390_at	**Hypothetical protein FLJ23598**	29.9	11p11.2
219508_at	Glucosaminyl (N-acetyl) transferase 3 (GCNT3)	13.9	15q21.3
205597_at	Chromosome 6 open reading frame 29 (C6orf29)	11.3	6p21.3
202357_s_at	B-factor (properdin)	11.3	6p21.3
220196_at	Mucin 16 (MUC16)	10.6	19q13.2
203186_s_at	**S100 calcium-binding protein A4 (S100A4)**	9.8	1q21
214456_x_at	Serum amyloid A1 (SAA1)	9.2	11p15.1
229927_at	LEM domain-containing 1 (LEMD1)	9.2	1q32.1
211848_s_at	Carcinoembryonic antigen-related cell adhesion molecule 7 (CEACAM7)	8.6	19q13.2
206199_at	Carcinoembryonic antigen-related cell adhesion molecule 7 (CEACAM7)	8.6	19q13.2
202917_s_at	S100 calcium-binding protein A8 (S100A8)	7.5	1q21
1555203_s_at	Chromosome 6 open reading frame 29 (C6orf29)	7.5	6p21.3
223179_at	**Yippee-like 3 (Drosophila) (YPEL3)**	7.0	16p11.2
204259_at	Matrix metalloproteinase 7 (MMP7)	7.0	11q21-q22
207076_s_at	Argininosuccinate synthetase (ASS)	7.0	9q34.1
201009_s_at	**Thioredoxin-interacting protein (TXNIP)**	6.5	1q21.1
226622_at	Mucin 20 (MUC20)	6.5	3q29
209183_s_at	**Hypothetical protein DKFZp564P1263**	6.5	10q11.21
242649_x_at	Chromosome 15 open reading frame 21	6.1	15q21.1
225283_at	Arrestin domain-containing 4 (ARRDC4)	6.1	15q26.3
201860_s_at	Plasminogen activator (PLAT)	5.7	8p12
226755_at	Unknown	5.7	---
201008_s_at	**Thioredoxin-interacting protein (TXNIP)**	5.3	1q21.1
226071_at	Thrombospondin repeat containing 1 (TSRC1)	5.3	1q21.2

Table II. Continued.

Probe set ID[a]	Gene[b]	Fold difference[c]	Chromosome[d]
225987_at	Tumor necrosis factor, α-induced protein 9 (TNFAIP9)	5.3	7q21.12
206421_s_at	Serine (or cysteine) proteinase inhibitor, clade B, member 7 (SERPINB7)	5.3	18q21.33
212531_at	Lipocalin 2 (LCN2)	5.3	9q34
218963_s_at	Keratin 23 (KRT23)	5.3	17q21.2
205563_at	**KiSS-1 metastasis-suppressor (KISS1)**	5.3	1q32
219529_at	Chloride intracellular channel 3 (CLIC3)	5.3	9q34.3
201010_s_at	**Thioredoxin-interacting protein (TXNIP)**	4.9	1q21.1
208170_s_at	**Tripartite motif-containing 31 (TRIM31)**	4.9	6p21.3
219795_at	Solute carrier family 6, member 14 (SLC6A14)	4.6	xq23-q24
209365_s_at	Extracellular matrix protein 1 (ECM1)	4.6	1q21
210029_at	Indoleamine-pyrrole 2,3 dioxygenase (INDO)	4.3	8p12-p11
202748_at	Guanylate-binding protein 2 (GBP2)	4.3	1p22.2
213693_s_at	Unknown	4.3	---
213172_at	Tetratricopeptide repeat domain 9 (TTC9)	4.0	14q24.2
219014_at	Placenta-specific 8 (PLAC8)	4.0	4q21.3
204885_s_at	Mesothelin (MSLN)	4.0	16p13.3
242907_at	Guanylate-binding protein 2 (GBP2)	4.0	1p22.2

[a]Probe set ID and gene description based on the assignment on the Affymetrix HG-U133 Plus 2.0 GeneChip (www.affymetrix.com). [b]The genes in bold print were further evaluated by RT-PCR. [c]Fold difference indicates the ratio of gene expression of LM-BxPC-3/BxPC-3. [d]Chromosomal location.

Table III. Liver metastasis after intrasplenic injection of parental BxPC-3 cells and S100A4 transfectants.

Cell line	Cell dose (cells/head)	Number of animal with liver metastasis[a] (metastasis/total)	Metastatic score in NOG mice	
		NOG	%T/L[b] (mean±SD)	Liver surface area[c] (mm^2, mean±SD)
BxPC-3	$1x10^5$	8/8 (100%)	2.8±1.5	434.5±35.0
Tf-clone B	$1x10^5$	5/5 (100%)	4.2±2.7	415.9±30.0
Tf-clone G	$1x10^5$	6/6 (100%)	20.2±10.8[d]	543.3±41.0
BxPC-3	$1x10^4$	1/8 (12.5%)	ND	ND
Tf-clone B	$1x10^4$	0/6 (0%)	ND	ND
Tf-clone G	$1x10^4$	3/6 (50%)	ND	ND

[a]Liver metastasis was evaluated 6 weeks after inoculation. [b]All liver images showing liver metastases in response to injection with $1x10^5$ cells were used to calculate the percent tumor occupancy in the liver (T/L). [c]The surface area of the liver was calculated using all liver images obtained from mice injected with $1x10^5$ cells. [d]$p<0.0001$ and $p=0.0006$ when compared with BxPC-3 and Tf-clone B, respectively. ND, not done.

in vitro growth activity and the expression levels of certain oncogenes were altered (17,20). In this study, we were able to establish a highly metastatic pancreatic cancer cell line, LM-BxPC-3, from a poorly metastatic parental cell line, BxPC-3, by a single passage in completely immuno-compromised NOG mice. The *in vitro* growth characteristics of the highly metastatic LM-BxPC-3 cell line did not differ from those of the parental cell line. Furthermore, neither cell line had mutations in the nucleotide sequences of the K and N-*ras* proto-oncogenes, but did carry the same mutation at

codon 27 of Ha-*ras* (CAT to CAC, His to His), and at codon 220 of the *p53* tumor suppressor gene (TAT to TGT, Tyr to Cys) (data not shown). Thus, while LM-BxPC-3 cells acquired a highly liver metastatic character, the *in vitro* growth characteristics and oncogene status of this cell line were similar to the parental cell line. These results suggest that our NOG model should permit molecular evaluation of the metastatic phenotype, including elucidation of putative genes associated with pancreatic cancer-liver metastasis. We used our metastatic model system to look for specific genes that may be involved in regulating liver metastasis. We screened LM-BxPC-3 cells and parental BxPC-3 cells for transcripts with at least a 4-fold difference in signal intensity between the highly metastatic cells and the parental cell line. Of the 47,000 transcripts analyzed, only 42 (0.09%) were expressed at ≥4-fold higher levels, and only 12 (0.03%) transcripts were expressed at ≥4-fold lower levels in LM-BxPC-3 cells compared with the parental cell line. A subset of nine genes was selected for validation of mRNA expression using real-time PCR, and the data was compared with the results from DNA chip analysis (Fig. 2j). In another method to corroborate the accuracy of our array data, genes that were identified many times, such as the regulator of G-protein signaling 4 (RGS4), parathyroid hormone-like hormone (PTHLH), thioredoxin-interacting protein (TXNIP), chromosome 6 open reading frame 29 (C6orf29), carcino-embryonic antigen-related cell adhesion molecule 7 (CEACAM7) and guanylate-binding protein 2 (GBP2), served as internal controls for reproducibility of the array data (Table II).

We identified 36 genes (42 probe sets) that were expressed at higher levels in LM-BxPC-3 cells than in parental BxPC-3 cells. These genes included several cell adhesion molecules, such as CEACAM7, extracellular matrix protein 1 (ECM1), matrix metalloproteinase 7 (MMP7), mucin family (MUC 16 and 20), and mesothelin (MSLN). These cellular components are important factors in the execution of metastatic potential and represent putative molecular targets for diagnostic/prognostic markers and gene therapy. However, we wanted to identify factors that were higher up in the hierarchy of metastatic regulation, i.e. upstream regulators of these execution factors. Therefore, we focused on genes encoding nucleoproteins and putative transcription factors, by looking for nuclear localization signals in the deduced amino acid sequences. The subcellular localizations of the putative proteins were predicted by PSORT (http://psort.ims.u-tokyo.ac.jp/) or PLOC (21), which are computer programs for predicting protein localization sites in cells. Four known (TRIM31, KISS1, YPEL3 and S100A4) and two novel genes (DFKZp56P1263 and FLJ23598) encoding putative nucleoproteins were validated by quantitative RT-PCR (22-25), in addition to three highly redundant genes (RGS4, PTHLH and TXNIP) that appeared three times in the array table (Table II). We were interested in identifying genes whose expression correlated with *in vivo* liver metastatic ability. At both the mRNA and protein levels, expression of S100A4 strongly correlated with *in vivo* liver metastatic ability in NOG mice. It is well known that the expression of S100A4 is associated with metastasis in several human solid carcinomas, including those of the bladder (26), breast (27), colon (28) and stomach (29), as well as melanoma (8). Overexpression of S100A4 has been shown to induce a metastatic phenotype in experimental rodent models of breast cancer (30,31), and transfection of the cDNA of S100A4 into a nonmetastatic rodent tumor cell line conferred a metastatic phenotype to the cells (32). The expression level of S100A4 seemed to influence tumor metastasis in our study as well, since there was a positive correlation between S100A4 expression (both at the level of mRNA and protein), and the liver metastatic potential of pancreatic cancer cell lines in the NOG mouse model. Down-regulation of S100A4 using hammerhead ribozymes or anti-sense RNA was shown to reduce *in vivo* metastatic potential and *in vitro* motility and invasive properties in a rodent model of osteosarcoma (33,34) and in the Lewis lung carcinoma model (35). Interferon-γ (IFN-γ) has been shown to suppress tumor cell growth *in vivo* and decrease the metastatic potential of several human cancer cell lines (36). The anti-tumor effects of IFN-γ are mediated in part by host-derived natural killer cells or macrophages. It has been shown that IFN-γ can downregulate the expression of S100A4, both at the mRNA and protein levels (37,38). Therefore, the anti-tumor activity of IFN-γ might be the result of a synergistic effect of activation of the host immune response and suppression of metastasis through downregulation of S100A4.

As mentioned above, the expression level of S100A4 closely correlated with the development of metastases in many human and rodent carcinomas. However, it is not clear how S100A4 expression was upregulated in these tumors. ERBB2 (*HER-2/neu*) upregulates expression of the S100A4 gene in human medulloblastoma cells via an ERBB2-responsive element located in the S100A4 promoter region (39). DNA methylation has also been shown to affect the expression of S100A4 in established cell lines and in primary pancreatic carcinomas (40-42). Treatment of benign rat mammary epithelial cells (Rama 37CL-A3) that express low levels of S100A4 with either of two demethylating agents, 5-azacytidine (5-aza-C) or S-adenosyl-L-homocysteine (SAH) resulted in a significant increase in the level of S100A4 mRNA. Furthermore, Southern blot analysis with a methylation-site-specific restriction enzyme showed different methylation patterns in the upstream region of the S100A4 gene in S100A4-low-expressing and -high-expressing benign rat mammary epithelial cells (41). The methylation status of two CpG sites in the first intron of the S100A4 gene has been associated with S100A4 expression in the human pancreatic cancer cell line Hs766T, because treatment of these cells with the demethylating agent 5-aza-2'-deoxycytidine (Decitabine) resulted in induction of expression of the S100A4 gene (40,42). These results strongly suggest that methylation of genomic DNA is, at least in part, responsible for repressing the expression of S100A4. Altered DNA methylation has been associated with carcinogenesis in a number of experimental systems (43,44). Thus, methylation/demethylation of genomic DNA is likely to be a mechanism for global control of gene expression.

S100 genes include at least 13 members, which are located in a cluster on chromosome 1q21 (45). Acquisition of 1q21-q23 has been associated with metastasis and a drug-resistant phenotype, particularly in sarcoma and ovarian cancer (46,47). Studies using comparative genomic hybrid-ization

(CGH) analysis indicated that a gain of chromosome 1 (1q21-23) often occurs in hepatocellular carcinoma and renal clear cell carcinomas (48,49). These data suggest that the long arm of chromosome 1, in particular 1q21-23, is important for the development of cancer and metastasis. Surprisingly, nine out of the forty-five genes we identified, based on differential expression between LM-BxPC-3 and parental BxPC-3 cells mapped to chromosome 1 (Table II). Moreover, six genes, including S100A4, S100A8, ECM1, TXNIP, thrombospondin repeat containing 1 (TSRC1) and RGS4 mapped to the 1q21-23 loci. We observed a similar pattern for several other differentially expressed genes, several of which were clustered in a single chromosomal locus: B-factor (properdin), TRIM31, and C6orf29 were located on chromosome 6p21.3; and lipocalin 2, arginino-succinate synthetase (ASS) and chloride intracellular channel 3 (CLIC3) were located on chromosome 9q34. These loci may be under global control as a locus control region (LCR), or may perhaps be regulated by genome-wide DNA methylation/demethylation or acetylation/deacetylation of the histone core.

In summary, we demonstrated that S100A4 gene expression in human pancreatic cancer cells correlated closely with *in vivo* liver metastatic ability, as evaluated in a quantitative model of metastasis in NOG mice. Our results suggest that S100A4 could be a potential therapeutic target in pancreatic carcinoma, in addition to being a molecular marker for diagnosis. Our quantitative model of metastasis in NOG mice is, of course, applicable to evaluation of the safety, efficacy, and medicinal benefits of new anticancer drugs.

Acknowledgements

We thank Dr J. Miyazaki (Osaka University, Japan) for providing the pCXN2 expression vector; and Kenji Kawai, Chie Yagihashi, and Hozumi Matsumoto for their excellent technical assistance.

References

1. Fidler IJ: The pathogenesis of cancer metastasis: the 'seed and soil' hypothesis revisited. Nat Rev Cancer 3: 453-458, 2003.
2. Giavazzi R, Campbell DE, Jessup JM, Cleary K and Fidler IJ: Metastatic behavior of tumor cells isolated from primary and metastatic human colorectal carcinomas implanted into different sites in nude mice. Cancer Res 46: 1928-1933, 1986.
3. Ikeda Y, Ezaki M, Hayashi I, Yasuda D, Nakayama K and Kono A: Establishment and characterization of human pancreatic cancer cell lines in tissue culture and in nude mice. Jpn J Cancer Res 81: 987-993, 1990.
4. Kuo TH, Kubota T, Nishibori H, *et al*: Experimental cancer chemotherapy using a liver metastatic model of human colon cancer transplanted into the spleen of severe combined immunodeficient mice. J Surg Oncol 52: 92-96, 1993.
5. Ohbo K, Suda T, Hashiyama M, *et al*: Modulation of hematopoiesis in mice with a truncated mutant of the interleukin-2 receptor gamma chain. Blood 87: 956-967, 1996.
6. Koyanagi Y, Tanaka Y, Kira J, *et al*: Primary human immunodeficiency virus type 1 viremia and central nervous system invasion in a novel hu-PBL-immunodeficient mouse strain. J Virol 71: 2417-2424, 1997.
7. Ito M, Hiramatsu H, Kobayashi K, *et al*: NOD/SCID/gamma(c)(null) mouse: an excellent recipient mouse model for engraftment of human cells. Blood 100: 3175-3182, 2002.
8. Ikoma N, Yamazaki H, Abe Y, *et al*: S100A4 expression with reduced E-cadherin expression predicts distant metastasis of human malignant melanoma cell lines in the NOD/SCID/γ_C^{null} (NOG) mouse model. Oncol Rep 14: 633-637, 2005.
9. Khatib AM, Fallavollita L, Wancewicz EV, Monia BP and Brodt P: Inhibition of hepatic endothelial E-selectin expression by C-raf antisense oligonucleotides blocks colorectal carcinoma liver metastasis. Cancer Res 62: 5393-5398, 2002.
10. Jain N, Thatte J, Braciale T, Ley K, O'Connell M and Lee JK: Local-pooled-error test for identifying differentially expressed genes with a small number of replicated microarrays. Bioinformatics 19: 1945-1951, 2003.
11. Niwa H, Yamamura K and Miyazaki J: Efficient selection for high-expression transfectants with a novel eukaryotic vector. Gene 108: 193-199, 1991.
12. Missiaglia E, Blaveri E, Terris B, *et al*: Analysis of gene expression in cancer cell lines identifies candidate markers for pancreatic tumorigenesis and metastasis. Int J Cancer 112: 100-112, 2004.
13. Han H, Bearss DJ, Browne LW, Calaluce R, Nagle RB and Von Hoff DD: Identification of differentially expressed genes in pancreatic cancer cells using cDNA microarray. Cancer Res 62: 2890-2896, 2002. Erratum in: Cancer Res 62: 4532, 2002.
14. Ryu B, Jones J, Blades NJ, Parmigiani G, Hollingsworth MA, Hruban RH and Kern SE: Relationships and differentially expressed genes among pancreatic cancers examined by large-scale serial analysis of gene expression. Cancer Res 62: 819-826, 2002.
15. Bresalier RS, Raper SE, Hujanen ES and Kim YS: A new animal model for human colon cancer metastasis. Int J Cancer 39: 625-630, 1987.
16. Nicholson BE, Frierson HF, Conaway MR, Seraj JM, Harding MA, Hampton GM and Theodorescu D: Profiling the evolution of human metastatic bladder cancer. Cancer Res 64: 7813-7821, 2004.
17. Nishimori H, Yasoshima T, Hata F, *et al*: A novel nude mouse model of liver metastasis and peritoneal dissemination from the same human pancreatic cancer line. Pancreas 24: 242-250, 2002.
18. Shishido T, Yasoshima T, Hirata K, *et al*: Establishment and characterization of human pancreatic carcinoma lines with a high metastatic potential in the liver of nude mice. Surg Today 29: 519-525, 1999.
19. Nomura H, Nishimori H, Yasoshima T, *et al*: A new liver metastatic and peritoneal dissemination model established from the same human pancreatic cancer cell line: analysis using cDNA macroarray. Clin Exp Metastasis 19: 391-399, 2002.
20. Gildea JJ, Golden WL, Harding MA and Theodorescu D: Genetic and phenotypic changes associated with the acquisition of tumorigenicity in human bladder cancer. Genes Chromosomes Cancer 27: 252-263, 2000.
21. Park KJ and Kanehisa M: Prediction of protein subcellular locations by support vector machines using compositions of amino acids and amino acid pairs. Bioinformatics 19: 1656-1663, 2003.
22. Dokmanovic M, Chang BD, Fang J and Roninson IB: Retinoid-induced growth arrest of breast carcinoma cells involves co-activation of multiple growth-inhibitory genes. Cancer Biol Ther 1: 24-27, 2002.
23. Lee JH and Welch DR: Suppression of metastasis in human breast carcinoma MDA-MB-435 cells after transfection with the metastasis suppressor gene, KiSS-1. Cancer Res 57: 2384-2387, 1997.
24. Hosono K, Sasaki T, Minoshima S and Shimizu N: Identification and characterization of a novel gene family YPEL in a wide spectrum of eukaryotic species. Gene 340: 31-43, 2004.
25. Heizmann CW, Fritz G and Schafer BW: S100 proteins: structure, functions and pathology. Front Biosci 7: d1356-d1368, 2002.
26. Davies BR, O'Donnell M, Durkan GC, Rudland PS, Barraclough R, Neal DE and Mellon JK: Expression of S100A4 protein is associated with metastasis and reduced survival in human bladder cancer. J Pathol 196: 292-299, 2002.
27. Rudland PS, Platt-Higgins A, Renshaw C, West CR, Winstanley JH, Robertson L and Barraclough R: Prognostic significance of the metastasis-inducing protein S100A4 (p9Ka) in human breast cancer. Cancer Res 60: 1595-1603, 2000.
28. Takenaga K, Nakanishi H, Wada K, Suzuki M, Matsuzaki O, Matsuura A and Endo H: Increased expression of S100A4, a metastasis-associated gene, in human colorectal adenocarcinomas. Clin Cancer Res 3: 2309-2316, 1997.
29. Yonemura Y, Endou Y, Kimura K, *et al*: Inverse expression of S100A4 and E-cadherin is associated with metastatic potential in gastric cancer. Clin Cancer Res 6: 4234-4242, 2000.

30. Grigorian M, Ambartsumian N, Lykkesfeldt AE, Bastholm L, Elling F, Georgiev G and Lukanidin E: Effect of mts1 (S100A4) expression on the progression of human breast cancer cells. Int J Cancer 67: 831-841, 1996.
31. Lloyd BH, Platt-Higgins A, Rudland PS and Barraclough R: Human S100A4 (p9Ka) induces the metastatic phenotype upon benign tumour cells. Oncogene 17: 465-473, 1998.
32. Levett D, Flecknell PA, Rudland PS, Barraclough R, Neal DE, Mellon JK and Davies BR: Transfection of S100A4 produces metastatic variants of an orthotopic model of bladder cancer. Am J Pathol 160: 693-700, 2002.
33. Maelandsmo GM, Hovig E, Skrede M, *et al*: Reversal of the *in vivo* metastatic phenotype of human tumor cells by an anti-CAPL (mts1) ribozyme. Cancer Res 56: 5490-5498, 1996.
34. Bjornland K, Winberg JO, Odegaard OT, *et al*: S100A4 involvement in metastasis: deregulation of matrix metalloproteinases and tissue inhibitors of matrix metalloproteinases in osteosarcoma cells transfected with an anti-S100A4 ribozyme. Cancer Res 59: 4702-4708, 1999.
35. Takenaga K, Nakamura Y and Sakiyama S: Expression of antisense RNA to S100A4 gene encoding an S100-related calcium-binding protein suppresses metastatic potential of high-metastatic Lewis lung carcinoma cells. Oncogene 14: 331-337, 1997.
36. Yanagihara K, Seyama T and Watanabe Y: Antitumor potential of interferon-gamma: retroviral expression of mouse interferon-gamma cDNA in two kinds of highly metastatic mouse tumor lines reduces their tumorigenicity. Nat Immun 13: 102-112, 1994.
37. Takenaga K: Suppression of metastasis-associated S100A4 gene expression by gamma-interferon in human colon adenocarcinoma cells. Br J Cancer 80: 127-132, 1999.
38. Andersen K, Smith-Sorensen B, Pedersen KB, Hovig E, Myklebost O, Fodstad O and Maelandsmo GM: Interferon-gamma suppresses S100A4 transcription independently of apoptosis or cell cycle arrest. Br J Cancer 88: 1995-2001, 2003.
39. Hernan R, Fasheh R, Calabrese C, *et al*: ERBB2 up-regulates S100A4 and several other prometastatic genes in medulloblastoma. Cancer Res 63: 140-148, 2003.
40. Rosty C, Ueki T, Argani P, *et al*: Overexpression of S100A4 in pancreatic ductal adenocarcinomas is associated with poor differentiation and DNA hypomethylation. Am J Pathol 160: 45-50, 2002.
41. Chen D, Rudland PS, Chen HL and Barraclough R: Differential reactivity of the rat S100A4(p9Ka) gene to sodium bisulfite is associated with differential levels of the S100A4 (p9Ka) mRNA in rat mammary epithelial cells. J Biol Chem 274: 2483-2491, 1999.
42. Sato N, Maitra A, Fukushima N, *et al*: Frequent hypomethylation of multiple genes overexpressed in pancreatic ductal adenocarcinoma. Cancer Res 63: 4158-4166, 2003.
43. Zingg JM and Jones PA: Genetic and epigenetic aspects of DNA methylation on genome expression, evolution, mutation and carcinogenesis. Carcinogenesis 18: 869-882, 1997.
44. Counts JL and Goodman JI: Alterations in DNA methylation may play a variety of roles in carcinogenesis. Cell 83: 13-15, 1995.
45. Engelkamp D, Schafer BW, Mattei MG, Erne P and Heizmann CW: Six S100 genes are clustered on human chromosome 1q21: identification of two genes coding for the two previously unreported calcium-binding proteins S100D and S100E. Proc Natl Acad Sci USA 90: 6547-6551, 1995.
46. Meza-Zepeda LA, Forus A, Lygren B, *et al*: Positional cloning identifies a novel cyclophilin as a candidate amplified oncogene in 1q21. Oncogene 21: 2261-2269, 2002.
47. Kudoh K, Takano M, Koshikawa T, *et al*: Gains of 1q21-q22 and 13q12-q14 are potential indicators for resistance to cisplatin-based chemotherapy in ovarian cancer patients. Clin Cancer Res 5: 2526-2531, 1999.
48. Wong N, Chan A, Lee SW, *et al*: Positional mapping for amplified DNA sequences on 1q21-q22 in hepatocellular carcinoma indicates candidate genes over-expression. J Hepatol 38: 298-306, 2003.
49. Gronwald J, Storkel S, Holtgreve-Grez H, *et al*: Comparison of DNA gains and losses in primary renal clear cell carcinomas and metastatic sites: importance of 1q and 3p copy number changes in metastatic events. Cancer Res 57: 481-487, 1997.